A MAP-BASED MODEL FOR THE DETERMINATION OF FUEL CONSUMPTION FOR INTERNAL COMBUSTION ENGINES AS A FUNCTION OF FLIGHT ALTITUDE

J. O. Kreyer, M. Müller, T. Esch
Department of Aerospace Engineering, FH Aachen UAS, Aachen, Germany

Summary

In addition to very high safety and reliability requirements, the design of internal combustion engines (ICE) in aviation focuses on economic efficiency. The objective must be to design the aircraft powertrain optimized for a specific flight mission with respect to fuel consumption and specific engine power. Against this background, expert tools provide valuable decision-making assistance for the customer.

In this paper, a mathematical calculation model for the fuel consumption of aircraft ICE is presented. This model enables the derivation of fuel consumption maps for different engine configurations. Depending on the flight conditions and based on these maps, the current and the integrated fuel consumption for freely definable flight emissions is calculated. For that purpose, an interpolation method is used, that has been optimized for accuracy and calculation time. The mission boundary conditions flight altitude and power requirement of the ICE form the basis for this calculation.
The mathematical fuel consumption model is embedded in a parent program. This parent program presents the simulated fuel consumption by means of an example flight mission for a representative airplane. The focus of the work is therefore on reproducing exact consumption data for flight operations.

By use of the empirical approaches according to Gagg-Farrar [1] the power and fuel consumption as a function of the flight altitude are determined. To substantiate this approaches, a 1-D ICE model based on the multi-physical simulation tool GT-Suite® has been created. This 1-D engine model offers the possibility to analyze the filling and gas change processes, the internal combustion as well as heat and friction losses for an ICE under altitude environmental conditions. Performance measurements on a dynamometer at sea level for a naturally aspirated ICE with a displacement of 1211 ccm used in an aviation aircraft has been done to validate the 1-D ICE model.

To check the plausibility of the empirical approaches with respect to the fuel consumption and performance adjustment for the flight altitude an analysis of the ICE efficiency chain of the 1-D engine model is done. In addition, a comparison of literature and manufacturer data with the simulation results is presented.

1. INTRODUCTION

In order to meet the targets set by the international community under the Paris Agreement for 2020, decarburization by reducing the combustion of fossil fuels in the transport sector is required. At the level of general aviation fuel reduction can be achieved by designing the aircraft and its powertrain to suit the flight application and the flight mission profile. To minimizing the take-off mass and the total energy requirement for a flight mission, the configuration of the powertrain in terms of the number, the position and maximum take off power of the necessary engines has to be taken under consideration. In addition, unconventional powertrain concepts such as hybridization or complete electrification are conceivable under consideration of the flight mission boundary conditions. A decision-maker who has to design the powertrain configuration for an aircraft is therefore faced with the difficult task of selecting the optimum powertrain with regard to flight mission boundary conditions and resource conservation.

Against this background, the research project "E-TAKE-OFF, Fliegen 2020" aims to provide a software-bound tool for the flight mission optimized dimensioning of aircraft and powertrain. This tool is intended to provide the buyer or owner of an aircraft with essential assistance in the selection and configuration. The project is limited to aircraft classes up to 5.7 t MTOM. The focus is on aircraft sizing and preliminary sizing.

The work package 3 (WP 3 ICE) described in this paper deals in particular with the modelling of the internal combustion engine (ICE) part of the powertrain. On the basis of the mission-specific energy demand, a fuel mass equivalent of the required fuel consumption will be calculated in addition to the dry weight for an engine. The simulation of the ICE drivetrain will be presented taking into account simulation accuracy and computing time. The simulation-based analysis of the fuel consumption for the required flight mission specific engine load points requires the inclusion of the flight altitude and the resulting environmental conditions.

The effect of the altitude influence on the ICE for flight and vehicle applications has already been investigated both simulatively and metrologically in various studies. In [1], Gagg and Ferrar propose a formula for calculating the

doi:10.25967/490162

change in power on the full load curve (full open throttle) for ICE as a function of altitude. Based on this, in [3] a numerical computational program is presented that shows the change of the full load power as a function of the variables: speed, intake pressure and ambient conditions, temperature and air pressure. In [4] and [5] two formulas for the calculation of the fuel consumption as a function of the take-of power or as a function of the volumetric efficiency, the effective mean pressure and other variables are presented. A comparable approach is also presented in the work of Donateo [2].

On the measurement side several test bench related investigations were carried out. Although the focus here is mostly on the investigation of the influence of altitude on the performance of combustion engines. Influences on fuel consumption have also been investigated, but were not the focus of the investigation. For turbocharged diesel engines with common rail direct injection, the following studies [6], [7] provide information on the influences. Here, effects such as a leaning of the mixture (increase of the air-fuel ratio) and an associated increase of the soot emission in combination with an increased fuel consumption at operating altitudes above 3000 m above sea level (SL). Physical effects such as an increase of the ignition delay and an associated increase of the exhaust gas temperature increased linearly with the operating altitude.

For passenger car gasoline engines, the question of fuel consumption as a function of altitude above 2000 m was raised in [8]. The results show no clear altitude dependence, since in [8] a complete vehicle test on a chassis dynamometer for different comparison cycles was not carried out. In studies dealing with passenger car consumption analyses, the authors typically orientate themselves on altitudes of up to 2200m, which corresponds to high-altitude cities such as Mexico City. A comparison for flight altitudes of small and medium passenger aircraft is thus not completely possible. In [9] the dependence of the operating altitude for the stationary load point operation of a four cylinder carburetor aircraft engine with a displacement of 1452 ccm was presented. The altitude conditions were simulated by changing the intake air pressure in front of the carburetor by air restrictors. The results show a sensitivity of the fuel consumption and the volumetric efficiency from the altitude or throttling. However, no detailed measurement data of the conditions (T, p, throttle angle) in the intake section of the engine are presented, which makes it difficult to interpret the results.

On the simulative side, one-dimensional (1-D) mathematical calculation models, i.e. dependent on time and one space coordinate, are largely used for the analysis of the height influence on the combustion engine process. The space coordinate refers to the description of the pipe flow in the inlet and outlet system of the combustion engine. In [10] a 1-D simulation of a turbocharged combustion engine with the simulation software Ricardo WAVE is presented. A statement is made about the performance and the consumption depending on the altitude. The simulation results show a very good agreement with the measured values recorded on a test bench. Unfortunately, no data sources are given, to make the measurement results interpretable for the power change after the altitude. A reference to the presented data is therefore critical. In [11] a 1-D engine model with the software GT-SUITE® of a ROTAX 914 engine is presented. In this paper, an analysis of the knocking behavior as a function of the flight altitude is simulative investigated. As a result formulas are presented to estimate the risk of knocking. The question of the knock influence as a function of the operating altitude for different fuels is also dealt with [12].

In general, it can be said that different authors have addressed the question of ICE performance as a function of altitude. With the exception of [5], however, no clear analytical formula relationships can be derived from the published sources that can be meaningfully integrated into a model environment. On a simulative level, 1-D combustion engine models are presented in order to analyze individual effects on the combustion process as a function of the influence of altitude. To the best of the authors' knowledge, a detailed investigation related to the efficiency chain has not yet been carried out.

2. OBJECTIVE

The project objective of E-TAKE-OFF, Fliegen 2020 is the determination of a powertrain configuration optimized for costs and consumption for a specific flight mission by providing an expert tool. On the one hand, the user of these expert tools relies on a high degree of accuracy in the calculation of the results. On the other hand, a high number of calculation operations is possible due to the high variance resulting from the different powertrain concepts. Within the third work package WP 3 ICE of the project a map-based methodology for the calculation of the load point and flight altitude dependent fuel consumption is presented. The programming of the methodology is implemented in the form of MATLAB® functions, which are integrated into a main program as submodels. The necessary map data are derived from a 1-D combustion engine simulation and validated on the basis of test bench test and literature data and stored in a library in the program. The developed submodels thus meet the boundary conditions required in the project with regard to computing speed and simulation accuracy.

The fuel consumption will be analyzed simulative for the combustion engine process by describing the efficiency loss chain. External influences related to environmental conditions, such as the thermodynamic state of the ambient air, are included in the analysis. Alternative metrological investigations in flight operations with the aim of energy balancing and efficiency investigations would entail high safety risks and are also costly. A multi-physical computer-assisted powertrain simulation is a sensible alternative, especially in the case of a high variety of variations. However, the simulative description of the specific fuel consumption for aircraft engines is computationally intensive due to complex non-linear relationships and error-prone if parameters are incorrectly set. For this reason, every form of simulation has to be validated or checked for plausibility against reliable data.

A wide variety of configurations are available on the market for aircraft engines. They differ, for example, in geometric engine characteristics such as the engine configuration (boxer, in-line engine, star and V-engine) and the engine-specific displacement. In addition, spark-ignited gasoline (AVGAS) and self-igniting kerosene (Jet A) engines are available on the market. To many other distinguishing

features, the pressure level of the charge (naturally aspirated or supercharged) is of particular characteristic importance for the engine description too. The aim of the project is to incorporate data on the greatest possible variety of combustion engine variants into the decision-making tool.

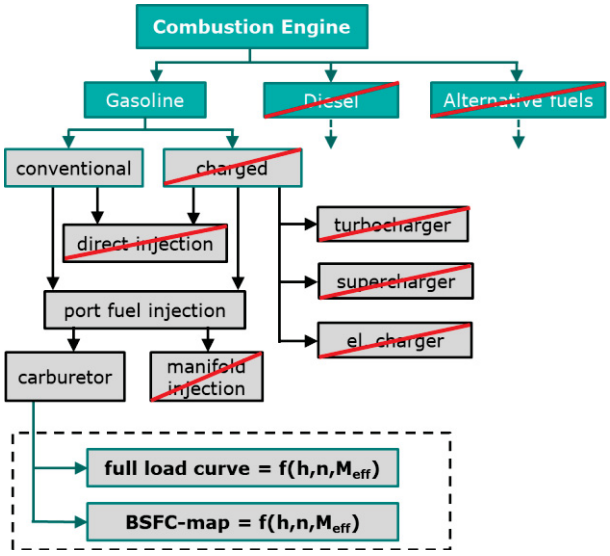

Figure 1: Aircraft engine configurations, limitations and simulation goals for WP 3 ICE

However, an exact description of the altitude flight and load point dependent fuel consumption for discrete stationary load points cannot be implemented seriously for the entire range of engine configurations within the framework of the project. For this reason, in the current project phase all modelling methods are presented using the example of a non-charged carburetor aircraft engine in the power range of 60 kW. Figure 1 gives an overview of the different configurations and shows the limitations as well as the goals that are currently present in the project.

3. ICE MODEL

After the objectives have been set out, this chapter will first explain the program structure of the simulation tool for the integration of the submodels for calculating fuel consumption (Chapter 3.1). In chapter 3.2 the interpolation method for the calculation of the load point dependent consumption from a break specific fuel consumption (BSFC) map will be discussed regarding calculation time and calculation accuracy. Chapter 3.3 introduces the method of height adjustment of the fuel consumption. Here it is explained in detail how on simulative level an adaptation of the BSFC maps is converted in dependence of the flight altitude. After a short introduction, the 1-D engine model created with the help of the GT-Suite® software is presented and the simulation results obtained are validated. Finally, the interpolation method and the method of altitude adjustment of the fuel consumption in the overall model are discussed using an example flight emission.

3.1: Presentation of the program structure of the simulation tool

Figure 2 shows the signal diagram of the model. Via the 'Parent Program' the engine configurations and the flight mission parameters are transferred to the submodels, which are responsible for the consumption calculation of the ICE. The calculation of a flight emission is divided into several phases: In an initialization phase, the maximum power requirement and the flight altitudes as well as the desired engine configuration are transferred to the submodel: 'ICE Map Generator'. In addition to the data for the dry mass and the installation space, this provides characteristic consumption maps. These data are either returned to the 'Parent Program' as fixed values for the flight emission course or, as in the case of the map data, made available for the second submodel: 'ICE Model'. During the mission simulation, mission conditions are transferred from the 'Parent Program' to the 'ICE Model' in fixed time steps Δt. The 'ICE Model' interpolates the BSFC in the required

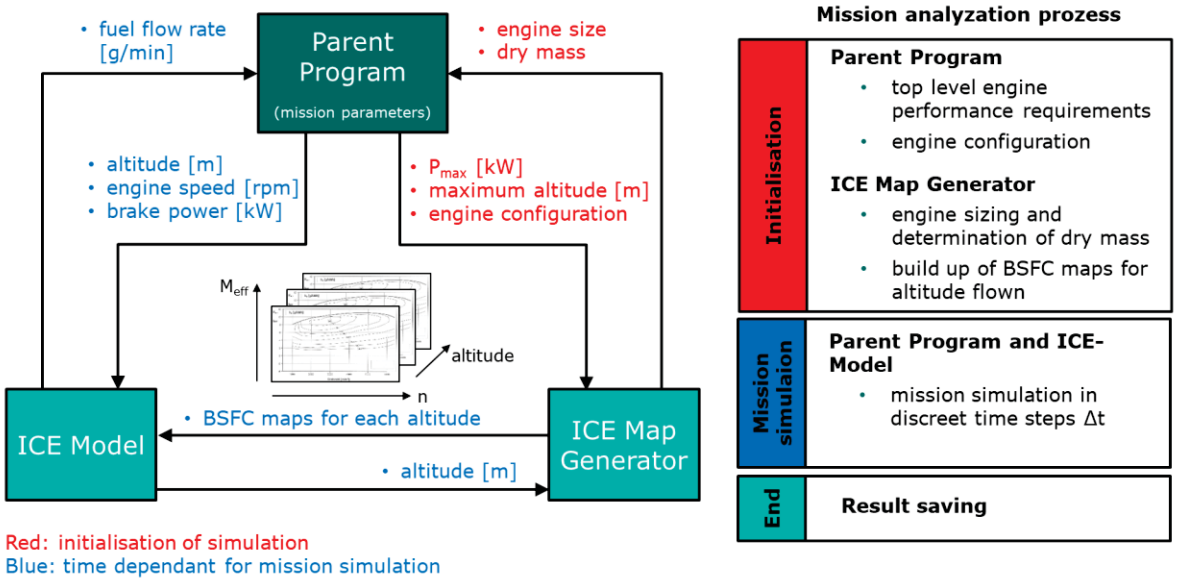

Figure 2: Signal diagram and program process

load point from the characteristic maps and gives the calculated fuel mass flow discretely in time back to the 'Parent Program'. After processing the data resulting from a mission analysis process, the 'Parent Program' runs through an optimization process and restarts the mission process with other configurations.

The model is designed so that only steady state engine states are calculated. A non stationary calculation (linear increase or decrease of load points, transient processes, etc.) is thus dispensed. For the derivation of the BSCF map data, this means that even only steady state engine states must be used with the aid of complex simulation models or test data. The demand on the subsystems 'ICE Map Generator' and 'ICE Model' in combination with the 'Patent Program' is thus defined as the time-discrete error-free calculation of stationary fuel consumption as a function of constant load and altitude requirements for ICE.

3.2: Discussion of the interpolation method for map data extraction:

Since speed and effective power are the input variables to the block: 'ICE Model', a map can be defined either by the effective torque or, if the displacement of the engine is known, also by the break mean effective pressure (BMEP). The output value is always calculated as fuel mass flow. The prerequisite for the functionality of the model block is the interpolation of the desired BSFC values in all engine operating ranges. Even if the load points along the characteristic propeller curve are decisive for flight operation, loadable grid points in the entire map range are necessary for interpolation. In principle, there are three ways to collect the characteristic maps of a motor: Research or provision of the data by the engine manufacturer, measurement on the test bench or post-simulation with appropriate software tools. Irrespective of the type of map data collection, in addition to the interpolation method, the quality of the grid points also has an influence on the correct reproduction of the consumption values. For this reason, several interpolation methods are tested and presented with regard to accuracy on thin and heavily populated maps as well as uniformly and unevenly gridded maps. In addition, the refraction duration of the methods is also evaluated. These methods are thus examined for the following categories:

- Accuracy of Reproduction
- Calculation effort for an interpolation step, related to time and computing power for a given CPU
- Influence of number and arrangement of grid points
- Reliability of extrapolation

The following methods have been selected for interpolation:

- Inverse Distance Weighting Interpolants (IDWI),
- Natural Neighbour Interpolant (NNI)

3.2.1: Inverse Distance Weighting Interpolanten (IDWI)

With this interpolation method, the point to be interpolated is calculated on the basis of the weighted distance squares to the grid points:

$$I_{IDWI}=\frac{\sum_{i=1}^{n}\frac{f(x_i,y_i)}{d_i^p}}{\sum_{i=1}^{n}\frac{1}{d_i^p}} \tag{3.1}$$

The IDWI method assumes that grid points exist in all directions around the interpolation point and that smooth surfaces exist in the definition space. For this reason, extrapolation is not possible. Smooth surfaces for a combustion engine BSFC map can be assumed, since no definition gaps are to be expected between the full load curve and the tractor curve of the engine as well as the speed limits.

For the IDWI, two types of interpolation data collection are tested:

- Circular Search Zone
- 4 Point Method

According to the IDWI circular search zone method, a large amount of data is collected around the interpolation point. Another disadvantage of this method is that it cannot distinguish between changing gradients. At turning points of the BSFC contour, too many grid points of a BSFC line are included in the calculation, depending on the location, and falsify the result. A remedy for this problem is the 4 Point Method. The next contour line in the four directions of the map axes along the coordinate system is searched from the interpolation point. An over determination of the same large grid points is avoided by this method.

3.2.2: Natural Neighbour Interpolation (NNI)

At the NNI the nearest subset of input values to an interpolation point is found and assigns a weight to these data proportional to calculated areas in order to interpolate the searched point [13]. This area calculation between the interpolation points is performed using Voronoi cells [14].

$$I_{NNI}(x,y)=\sum_{i=1}^{n} f(x_i,y_i)\cdot w_i(x,y) \tag{3.2}$$

$$w_i(x,y)=\frac{A(x_i,y_i)}{A(x,y)} \tag{3.3}$$

Here $I_{NNI}(x,y)$ is the interpolation value at the searched location x,y. $f(x_i,y_i)$ is the given data and $w_i(x,y)$ is the weightings per data point calculated over the assigned areas. The method avoids trends and gaps in definitions. The generated surfaces in which the data is interpolated are connected to the grid points and are flat (see Figure 3).

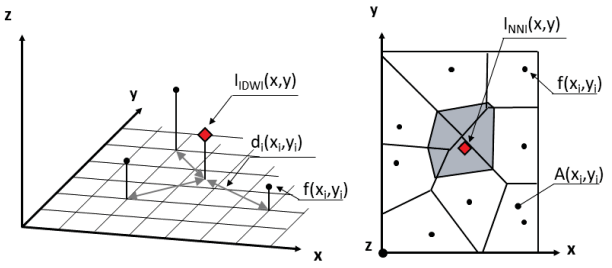

Figure 3: Interpolation methods. Left: Inverse Distance Weighting Interpolanten (IDWI); right: Natural Neighbour Interpolation (NNI)

Compared to the IDWI, weights of the grid points are assigned according to their percentage area overlap and not only according to their distance.

In the first step, the interpolation methods are checked against each other on a test BSFC map. The fuel consumption isolines of the test map from 245 g/kWh to 500 g/kWh with a fixed grid of ΔBMEP = 0.03 bar and Δn = 10 rpm were digitized from a bidmap file. The digital data set was examined at seven test sites.

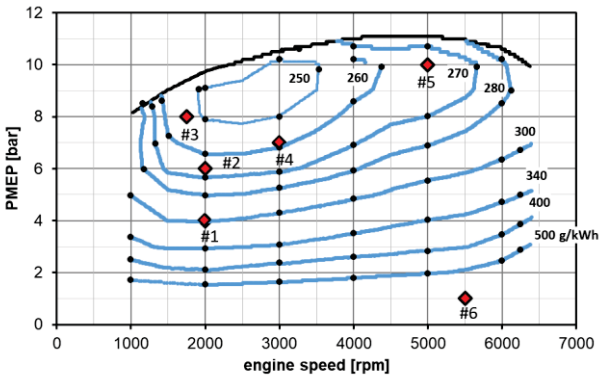

Figure 4: Test BSFC map: The black line is the full load curve. The blue points are iso BSFC values with a grid of ΔBMEP = 0.03 bar and Δn = 10 rpm. The black points are iso BSFC values lesser meshed but evenly distributed according to the engine speed.

In a direct comparison of the interpolation methods, the IDWI - Circular Search Zone has the best computing time, but leads to the most inaccurate results. The load points 2 to 5 are estimated insufficiently according to the values of the isolines. Extrapolation is not possible. The IDWI - 4 point for a significant improvement of the interpolation results, but the computational effort also increases. A meaningful extrapolation is not given. The NNI method has the most accurate interpolation results measured against the expected BSFC values, is extrapolatable and can be used with a computing time of less than 1.3 s on a computer with 3,7 GHz processor. Thus, this method was implemented in the ICE model.

In a second step, a comparison for the interpolation quality for the NNI method is made between a close meshed map (blue points in figure 4) that provides data on the iso BSFC lines and an lesser meshed map that is evenly distributed according to the engine speed (black points in figure 4). It is noticeable that the lesser meshed shows depending on the point less accurate than the close meshed map (compare point #3). However, less data is needed which is in favor of the computing time. For optimal use of NNI, a closely meshed map with equal spacing should therefore be provided.

3.3: Presentation of the method for height adjustment of consumption maps:

This chapter explains and validates the 1-D engine simulation with all technical details.

3.3.1: Technical and physical basics

In addition to changes in external physical boundary conditions such as weather-related ambient pressure, ambient temperature and humidity, control measures by pilots or engine controllers also have an influence on fuel consumption. In conventional spark ignition aviation ICE, load control is carried out via several control and regulation devices:

- Throttling the intake gaseous mixture
- Adjustment of the ignition timing
- Setting the mixture quality (Leaning)
- Cowl flap opening

The last point has to do with ensuring sufficient cooling. With regard to the altitude adjustment, the ignition timing and the pressure level present in the engine inlet must be adjusted to prevent abnormal combustion (e.g. knocking) on the one hand and to keep the air-fuel ratio within the ignition limits on the other. In addition, the density of the unburned mixture in the cylinder has an influence on the burning speed so that an adaptation of the ignition timing to the altitude flight is necessary.

As the air density decreases with altitude, the filling of the engine with fresh gas and thus also the performance of the

			IDWI - Circular Search zone		IDWI - 4 Point		Natural Neighbour Interpolant			
			results based on blue points in figure 4						results based on black points in figure 4	
#	n [rpm]	BMEP [bar]	BSFC [g/kWh]	Calc. time [s]	BSFC [g/kWh]	Calc. time [s]	BSFC [g/kWh]	Calc. time [s]	BSFC [g/kWh]	Calc. time [s]
1	2000	4	300,00	0,258	300	0,274	299,20	1,266	301,02	0,387
2	2000	6	270,00	0,289	263,03	3,581	266,93	0,984	266,18	0,287
3	1750	8	250,00	0,4	253,18	5,9	255,79	1,016	270,06	0,367
4	3000	7	250,00	0,7	260	0,9	259,43	0,984	258,40	0,294
5	5000	10	270,00	0,8	268,73	3,9	270,00	1,078	270,00	0,309
6	5500	1	481,29	1	500	6	602,52	1,031	630,04	0,355

Table 1: Results of interpolation methods tested on a computer with a 3,7 GHz processor

engine must be expected to decrease. An analytical description of the reduction of the effective power at the full load line is given in [1] on the density ratio of the intake air with respect to the sea level (SL).

(3.4) $$\frac{P_{eff}}{P_{eff,\,SL}} = \sigma - \frac{1-\sigma}{7{,}55} \qquad \text{with } \sigma = \frac{\rho}{\rho_{SL}}$$

Mises [5] also presents an analytical formula for calculating the BSFC dependent on ambient conditions:

(3.5) $$BSFC(\sigma) = 639907{,}18 \cdot \frac{F(\sigma) \cdot \lambda_a}{\lambda \cdot BMEP}$$

(3.6) $$F(\sigma) = \frac{0{,}935 \cdot \sigma}{\sigma^{1{,}117} - 0{,}065}$$

In formula (3.5), in addition to the function F(σ), the volumetric efficiency λ_a, the air-fuel ratio λ and BMEP must be given. Thus a derivation of these quantities is necessary for a certain engine type in dependence of the flight altitude in each case. On way to analyze the fuel consumption is by describing the energy loss chain. According to [15] the losses for spark-ignited engines can be classified according to the following categories:

- Losses due to non-ideal combustion
- charge exchange losses
- leakages
- friction
- wall heat losses

The control functions and the loss mechanisms are interlinked. For example, the charge exchange losses are reduced when the throttle valve is opened at full load. However, environmental influences also affect the loss path in a variety of ways. One example here is the evaporation of the fuel in the intake manifold (fuel-mixture generation).

In summary, the scope of the simulation must have a modelling depth that includes all the control devices on the one hand and describes the physical relationships sufficiently precisely on the other.

3.3.2: GT Model

The height influence calculation is carried out using the simulation of the ROTAX 912UL engine. The four-cylinder, water/air-cooled and carburetor-controlled aircraft engine has a displacement of 1211.12 ccm and a maximum take-off power of 59.6 kW at a speed of 5800 rpm. The engine was measured stationary on the propeller test bench of the Fachhochschule Aachen, to form a basis for validation.

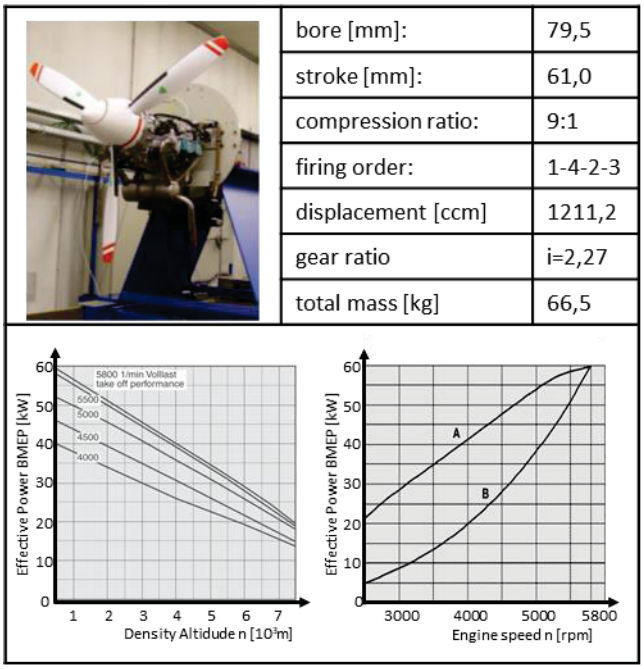

Figure 6: Data of the ROTAX 912 UL [16]. Right map: A full load curve, B propeller curve.

The created simulation model is divided into several interconnected elements (see Figure 5). GT-Suite® provides for each typical engine element a template. The core templates to be parameterized are the fluid lines for fresh gas and exhaust gas, the inlet and outlet valves, the combustion chamber and the engine kinematics. The carburetor model is not given as a template and is designed out of other elements provides in the GT-Suite® library. Since fluid lines and carburetor model are necessary for the simulation of mixture preparation and gas dynamics, the actual combustion simulation is performed the template: 'EngCylinder'. Upstream and downstream the 'EngCylinder' are the 'ValveCamConn' templates used for the mechanical and gas dynamic description of the inlet and outlet valves. 'EngineCrankTrain' requires the mass and the moment of

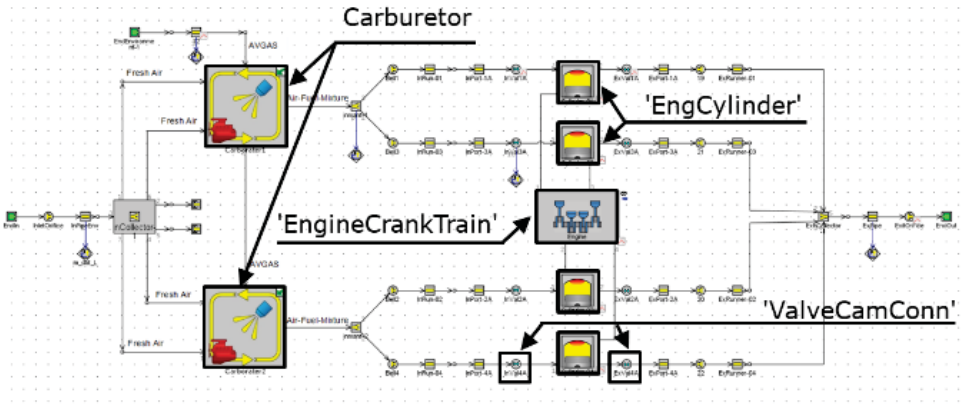

Figure 5: GT-Suite® ROTAX 912 UL engine model

inertia of the crankshaft, connecting rods and pistons as parameters besides other geometry data. The 'EngineCrankTrain' contains the Chen-Flynn engine friction model, which indicates the friction losses as a function of pressure and engine speed parameters. A detailed description of the parameterization is given in [17].

The fluid lines have been geometrically measured at the engine according to length, diameter, wall thickness and radii. GT calculates the Navier-Stokes equations for each line element to determine the vectorial and scalar state variables of the respective fluid. The necessary material data to determine the thermophysical fluid properties are stored in a library.

The carburetor model has been developed on mechanical as well as thermodynamic and fluid dynamic level. It has the task to model the mixture formation depending on a stationary load request via the throttle position and to adjust the engine to the desired load point. The individual elements of the carburetor are shown in Figure 7. In the carburetor model, the kinematics of the control nozzle, which is controlled via the upper and lower chamber, are calculated by means of the applied force equilibrium.

$$(3.7) \qquad A_2 \cdot p_u - A_1 \cdot p_1 - c_s \cdot (y + y_0) - m \cdot \ddot{y} = 0$$

The inflow of fuel and ambient air into the mixing chamber is calculated using the throttle equation as a function of the fluid densities and pressure differences.

$$(3.8) \qquad \dot{m}_{F,i} = \mu_{D,i} \cdot A_{D,i} \cdot \sqrt{\frac{2}{\rho_{u,i}}} \cdot \sqrt{p_u - p_1} \cdot \rho_{u,i}$$

$$(3.9) \qquad \dot{m}_{TP} = \frac{\mu_{TP} \cdot A_{TP}(\varphi) \cdot p_1}{\sqrt{R_L T_1}} \left(\frac{p_2}{p_1}\right)^{1/\kappa_1} \left\{ \frac{2\kappa_1}{\kappa_1 - 1} \left[1 - \left(\frac{p_2}{p_1}\right)^{(\kappa_1 - 1)/\kappa_1} \right] \right\}^{0,5}$$

The equation (3.9) according to [18] is used to calculate the flow of the air-fuel mixture through the throttle valve. In [18] the function for determining the geometric opening cross section at the throttle valve $A_{TP}(\varphi)$ as a function of the opening angle is also presented. All geometric and mechanical data were measured on a carburetor of identical design. However, the respective flow coefficients: μ_{TP}, $\mu_{D,i}$, could not be measured. They were adjusted iteratively by comparisons with test bench data as a function of opening angle or geometric cross-sectional area. The flow coefficient μ_{TP} of the throttle valve as a function of the throttle angle is shown in Figure 8.

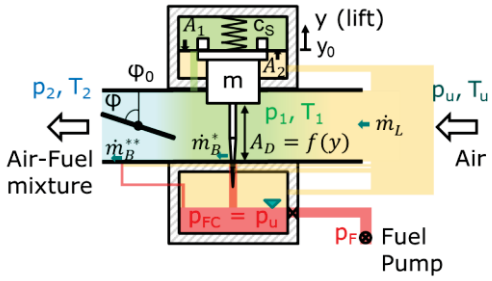

Figure 7: Carburetor model design

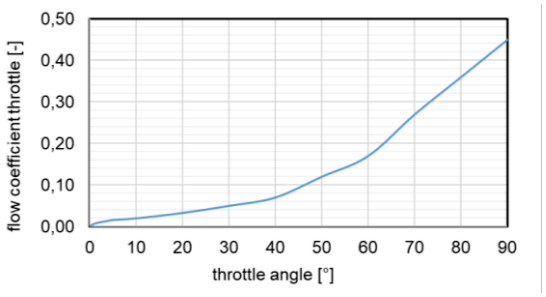

Figure 8: Flow coefficient throttle plate carburetor

The core of the multi-physical simulation of an ICE is the modeling of the combustion process in the combustion chamber. One possibility is the 1-zone cylinder model. In this case, a mass and energy balance is carried out in a control volume describing the combustion chamber and neglecting the conservation of impulses. In Figure 9 the mass and energy balances to be calculated for a 1-zone combustion chamber model are visualized. Additional details on the engine process calculation can be found in [15], [19].

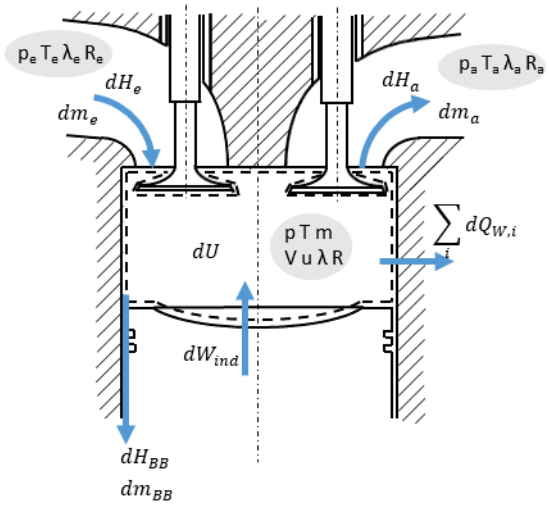

Figure 9: Model of combustion chamber analysis with state variables and energy and mass flows

The mass balance for the 1-zone model puts the masses entering and exiting the volume into proportion:

$$(3.10) \qquad \frac{dm_{sys}}{dt} = \frac{dm_e}{dt} + \frac{dm_a}{dt} + \frac{dm_{BB}}{dt} + \frac{dm_{Br,ved}}{dt}$$

The energy balance of the 1-zone model describes the differential change in the internal energy of the balance system stored in the combustion chamber as a result of the inflow and outflow of other energies over time:

$$(3.11) \qquad \frac{dE_{sys}}{dt} = \frac{dU}{dt} = \frac{dQ_B}{dt} + \frac{dQ_W}{dt} + \frac{dm_e}{dt} \cdot h_e + \frac{dm_a}{dt} \cdot h_a + \frac{dm_{BB}}{dt} \cdot h_{BB}$$

$$-(p - p_u) \cdot \frac{dV}{dt} + \frac{dm_{Br,verd}}{dt} \cdot h_{Br,verd} + \frac{dQ_{ver}}{dt}$$

The detailed description of the terms in equations (3.10) and (3.11) gives an overview of the most important

parameters to be defined which are required by the engine model.

Description of terms $\frac{dm_{e,a}}{dt}\cdot h_{e,a}$. Charge exchange:

The inflow and outflow of gaseous fluids via the inlet and outlet valves are subject to throttling and frictional influences. The real mass flow rate can be calculated using a flow coefficient dependent on the valve lift and a theoretical isentropic mass flow rate using the flow function:

(3.12) $$\dot{m}_{in}=\mu\cdot\dot{m}_{theo}$$

(3.13) $$\dot{m}_{theo}=A_{geo}(h_V)\cdot\sqrt{p_{in}\cdot\rho_{in}}\cdot\Psi\left(\frac{p_{in}}{p},\kappa\right)$$

(3.14) $$\Psi=\sqrt{\frac{2\cdot\kappa_{in}}{\kappa_{in}-1}\cdot\left[\left(\frac{p_{in}}{p}\right)^{\frac{2}{\kappa_{in}}}-\left(\frac{p_{in}}{p}\right)^{\frac{\kappa_{in}+1}{\kappa_{in}}}\right]}$$

For this purpose, the flow coefficient μ and the geometric valve cross section A_{geo} must be determined as a function of the valve lift. In addition the isentropic exponent as a function of the quality of the fresh gas respectively the exhaust gas must be derived.

(3.15) $$\kappa=-\frac{\frac{dp}{p}}{\frac{dv}{v}}$$

While κ is determined numerically by substance databases as a function of the mixture composition and its thermodynamic state, the flow coefficient must be investigated on the basis of simulative (e.g. 3-D CFD) or measurement investigations (e.g. flow bench). Since there were no possibilities for either method, the flow coefficient was adapted to similar inlet and outlet channels and valve geometries (Figure 10 and 11). The maximum valve lift and the valve timing of the Rotax 912 UL were adapted to the program. The exact cam profile was not measured, so an approximated cam profile was used.

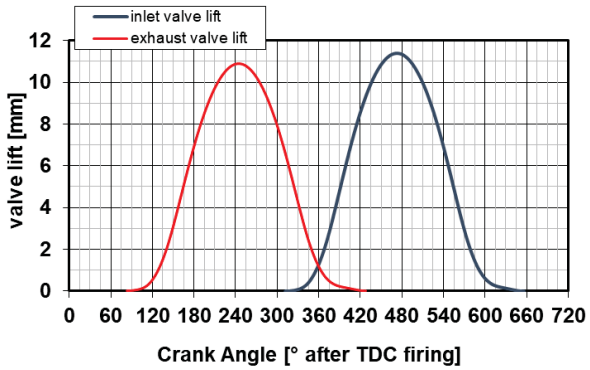

Figure 10: Valve timing and valve lift for inlet and exhaust valves

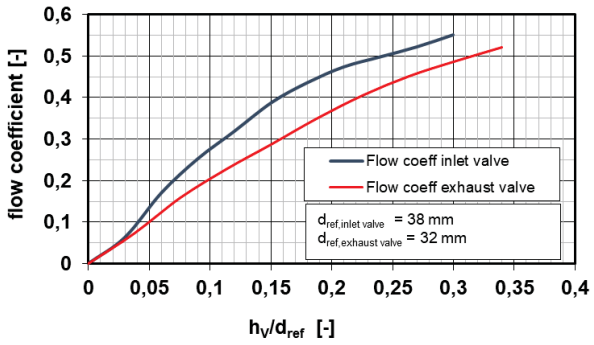

Figure 11: Flow coefficient as a function of valve lift relative to the reference diameter d_{ref} of the valve

Description of the term: $\frac{dQ_B}{dt}$. Combustion model:

The combustion model describes the energy release in the combustion chamber (burn rate). The mathematical modelling for calculating the heat release from the fuel $\frac{dQ_B}{dt}$ is described by the following burn rate function according to Vibe:

(3.16) $$Q_B(\varphi)=\eta_{complete}\cdot\left(1-e^{-x_{awb}\left(\varphi-\varphi_{BB}\right)^{m+1}}\right)$$

The Vibe exponent m and the combustion efficiency $\eta_{complete}$ define the quantity of the burned fuel against time and piston position. The angle between start of combustion and top dead center of the ignition φ_{BB} is calculated as a function of the Vibe exponent m, the burning duration and the Anchor Angel. These three values can be used to adjust the shape of the burning process. This makes the simulation independent of a value for the ignition timing which is not implemented in the model. A modelling of a knocking combustion is also not included.

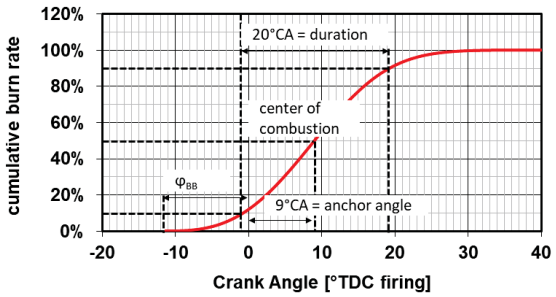

Figure 12: Fuel burn rate at SL application

Description of the term: $\frac{dm_{Br,verd}}{dt}$. Evaporation model:

The evaporation of the fuel is described using an empirical evaporation model:

(3.17) $$\frac{dm_i}{dt}=-\frac{4{,}16\cdot n_{ref}}{CA50}\cdot\left(\frac{T}{T_{ref}}\right)\cdot\left(\frac{n}{n_{ref}}\right)\cdot m_i$$

The reference temperature T_{ref} is set to 600 K and the reference motor speed n_{ref} to 4000 rpm. CA50 is the crank angle value when 50 % of fuel is evaporated.

Description of the term: $\frac{dW_{ind}}{dt}$. Mechanical work:

The description of the power delivered by the piston is calculated by the volume change multiplied by the difference between the cylinder pressure p and the crankcase pressure p_u which is set to environmental conditions:

(3.18) $$\frac{dW_{ind}}{dt}=(p_u-p)\cdot\frac{dV}{dt}=(p_u-p)\cdot\omega\cdot\frac{dV}{d\varphi}$$

Description of the term: $\frac{dQ_W}{dt}$. Heat losses:

Newton's law of cooling is used to describe the heat transfer from the combustion chamber to the environment. For the heat losses, the following three paths are possible:

- Heat convection into the cylinder walls
- Heat convection into the cooling water via the cylinder head
- Heat convection into the oil via the piston cup, the piston skirt and the piston rings

The sum of these heat flows describes the total process-related heat loss flow from the combustion chamber:

(3.19) $$\frac{dQ_{W,i}}{dt}=\sum_i \alpha_i\cdot A_i\cdot\left(T_{w,i}-T_{Gas}\right)$$

The paths are visualized in Figure 13. The wall temperatures $T_{w,i}$ of the component are the interior wall temperatures in the direction of the combustion chamber, which are given as functions of location and time. For the modelling of the engine, however, no separate model of the cooling circuit has been constructed. The conditions for the temperature of the cooling water, the oil and the environment are taken from input templates or set to be constant. These fluid temperatures must therefore be specified as functions of the height. In addition, the heat transfer coefficients α_i from the combustion chamber to the walls must be defined. The heat convection between the gas and the combustion chamber wall component are modelled in GT-Suite® using semi-empirical approaches according to Woschni [17], [18], [19]. Although a split cooling concept is available, for the simulation, the heat flow through the cylinder walls is completely dissipated to the environment by the cooling fins. For this, an additional heat transfer coefficient from the cylinder wall to the environment has to be defined.

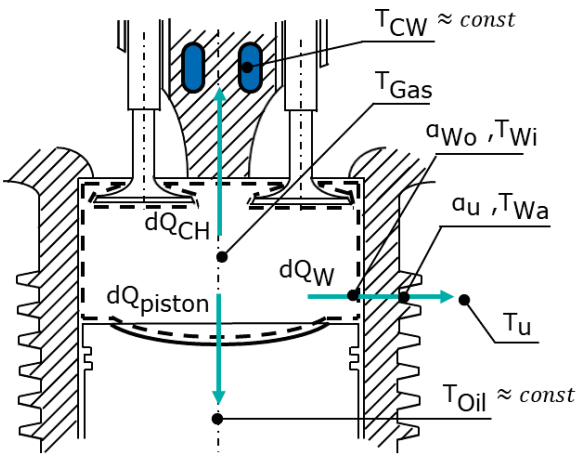

Figure 13: Heat transfer model

The cooling, whether by flow around the cylinder cooling fins or by discharge through a radiator, depends strongly on the flow around the engine and the flow of ambient air through the cowling. An approach for determining the cooling capacity for aircraft ICE can be found in [20]. Here, based on the NACA cooling correlation method, a balancing model for determining the cooling capacity is presented and validated on the basis of flight measurement data. The following polynomial approach relates the indicated engine power, the exhaust gas temperature and the cylinder wall temperature to the density and temperature of the ambient air for a defined cooling air mass flow.

(3.20) $$\frac{c\cdot P_i^{\,m}}{(\sigma\cdot\Delta p)^n}=\frac{T_w-T_u(h)}{T_{ex}-T_u(h)}=\zeta$$

Here σ again stands for the density ratio of the ambient air at flight altitude in relation to the sea level (see chapter 3.3.1). Δp is the pressure loss due to the cowling of the engine and the coefficients m, n and c depend on the geometry of the engine. The correlation applies to flight altitudes up to 6000 m and was well confirmed in flight tests with a Gulfstream Aerospace Corporation Commander 700 with two Lycoming TI0 540 R2AD turbocharged engines.

Assuming a constant heat flux from the combustion chamber via the cylinder wall into the environment and neglecting the heat conduction through the cylinder wall in which $T_{Wi} = T_{Wa} = T_W$ is set, the necessary derivation of heat transfer coefficients is possible. This rough simplification allows to establish a correlation between the inner cylindrical heat transfer coefficient according to Woschni α_{Wo} in relation to the convective heat transfer coefficient at the fluted outer wall of the cylinder α_u.

(3.21) $$\frac{\alpha_u}{\alpha_{Wo}}=\frac{T_{ex}-T_W}{T_W-T_u(h)}$$

By transforming equation 3.20 into equation 3.21 and eliminating the wall temperature T_W, an altitude dependent correlation for estimating the heat transfer coefficient to the cooling water can be established and implemented in the model:

(3.22) $$\frac{\alpha_u}{\alpha_{Wo}}=\frac{T_{zyl}\cdot(1-\zeta)+T_u(h)\cdot(\zeta-1)}{\zeta\cdot(T_{zyl}-T_u(h))}$$

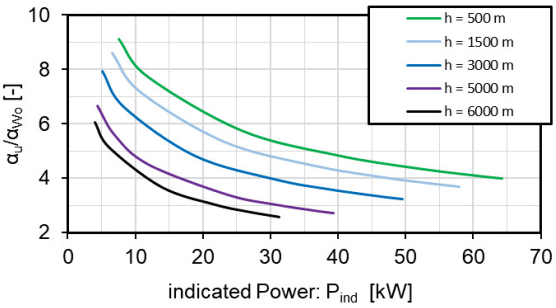

Figure 14: calculated ratio between the heat transfer coefficients inside and outside the cylinder

The coefficients m=0.33, n=0.3 and c=0.473 from [20] were used for the evaluation. In addition, a constant pressure loss Δp = 2000 Pa was used as a mean value. The coefficients are of course geometry dependent and Δp and therefore the mass flow rate of cooling air is also dependent on the flight speed and the flight altitude. In [20] these values were determined by measurement and calculation and are thus in a meaningful connection. The exhaust gas temperature, the heat transfer coefficient according to Woschni and the indicated power are selected for the stationary load points in the model. Based on this the ratio for heat transfer coefficients as a function of altitude can be defined. Figure 14 is a representation of the simulation results.

Description of the term: $\frac{dm_{BB}}{dt} \cdot h_{BB}$ and $\frac{dQ_{ver}}{dt}$. Energy losses:

$\frac{dm_{BB}}{dt} \cdot h_{BB}$ and $\frac{dQ_{ver}}{dt}$ describe the blow-by losses of gas from the cylinder and other heat losses. These are relatively small and have been neglected.

3.3.3: Model validation on see level:

To check the accuracy of the 1-D simulation model, the simulation results are compared against test bench measurements. The ROTAX 912UL was measured on a test bench in the engine laboratories of the Aachen University of Applied Sciences along the propeller curve shown in Figure 15 at stationary load points. The BSFC map was derived from the simulated points using the MATLAB® App: Curve fitting Tool. The Thin-plate spline method was used for data extrapolation [21]. The measurement results and the corresponding simulation results for the load points 1 to 7 as well as the calculated relative deviations can be seen in Figure 16. The results showed that, with the exception of load point #2, there is a relative error of maximum 10% between simulation and measured value.

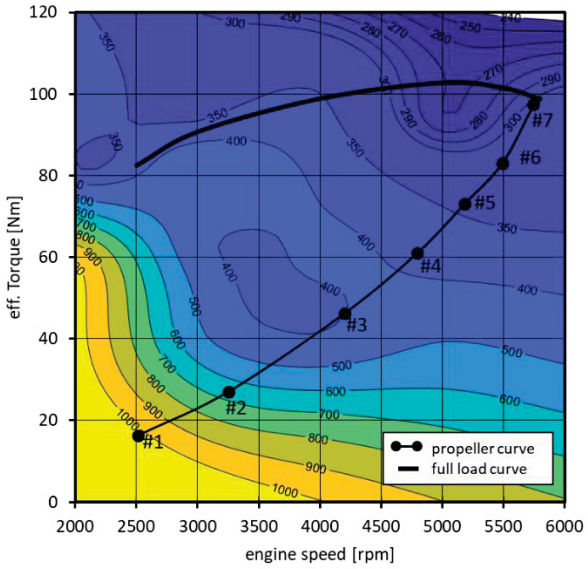

Figure 15: BSFC Map of the ROTAX 912UL simulation model for see level operation. Points on the propeller curve are measured values on the engine dyno

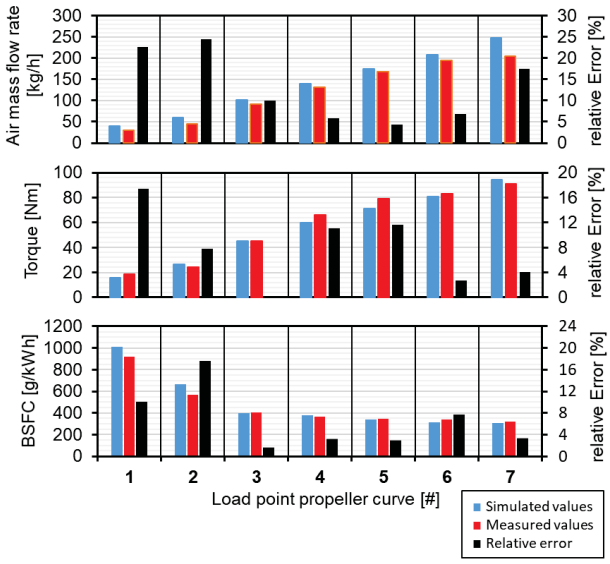

Figure 16: Simulation and measurement results for steady state load points on the propeller curve

The simulation results in the form of a BSFC map for the altitude flight at 3000 m can be found in Figure 17. The full load curve shown there has been calculated on the basis of the full load curve using the calculation method according to Gagg Ferrar [1]. Within the 1-D engine simulation the maximum achievable load points at the full load curve have been simulated. As can be seen in Figure 17, these points roughly correspond to the full load line that can be reached via the full load line proposed by Gagg Ferrar.

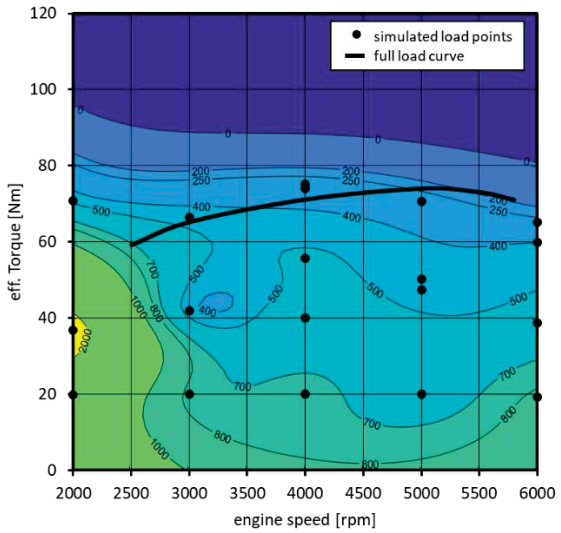

Figure 17: BSFC Map of the ROTAX 912UL simulation model for 3000 m operation

In order to be able to evaluate the simulation results, no measurement data could be collected. For this reason data have been taken from a flight manual of Diamond Aircraft (DA 20 Katana) [22]. The fuel consumptions for the power settings in cruise flight at an altitude of 3000 m and 4000 m, which result from the manual, are compared with the corresponding simulation results in table 2. It should be noted that fuel mass flows are tabulated in [22]. On the basis of the spread of the possible fuel density, maximum and minimum fuel consumption result for the load points. These coincide with the simulated data for the high load point near the full load curve with a deviation of approx. 4 % BSFC. At the lower speed load point there is a deviation of the BSFC value of approx. 35 %.

	Reference Data Flight Manual [22]				Simul-ation
h	n	M_{eff}	BSFC @ ρ_{AVGAS} 0,73 kg/l	BSFC @ ρ_{AVGAS} 0,78 kg/l	BSFC
[m]	[U/min]	[Nm]	[g/kWh]	[g/kWh]	[g/kWh]
3000	4772,67	63,82	281,47	300,75	409
	5454,48	66,00	280,77	300,00	312
4000	5227,21	58,28	281,47	300,75	345

Table 2: Comparison of simulation data and flight manual data for a flight altitude of 3000 m and 4000 m

4. SUMMARY AND OUTLOOK

In this paper a method for the map-based calculation of the flight altitude dependent fuel consumption of ICE is presented. The aim of this method is to calculate fast and reliable fuel consumption values for stationary engine conditions. For this the numerical interpolation from iso gridded BSFC maps according to the Natural Neighbor Interpolation (NNI) was identified as the most efficient method. The provision of the map data is performed by a multi-physical 1-D engine simulation. After the definition and the parameterization of the engine parameters required for the simulation, it is possible to derive resilient BSFC map data for sea level environmental conditions as well as for high-altitude flight. This is shown by the validation with test bench and literature data. In the next steps an extension of the map data is planned for the simulation of a turbocharged aircraft engine in the power class of 105 kW MTOP.

REFERENCES

[1]: Gagg, R.F., Farrar, E.V., “Altitude Performance of Aircraft Engines Equipped with Gear-Driven Superchargers,” SAE Jour.,Vol. 34, No. 6, June 1934, pp. 217-25, doi:10.4271/340096.

[2]: Donateo, T. and Ficarella, A., "Designing a Hybrid Electric Powertrain for an Unmanned Aircraft with a Commercial Optimization Software," SAE Int. J. Aerosp. 10(1):2017, doi:10.4271/2017-01-9000

[3]: Smith, H. C., Dreier, M. E., „A Computer Technique for the Determination of Brake Horsepower Output of Normally-Aspirated Reciprocating Aircraft Engines“, SAE 770465

[4]: Farokhi, S.; “Aircraft Propulsion”, John Wiley & Sons, 2014.

[5]: Mises, R.V., „Theory of Flight“, Dover, Toronto 1059, p. 362

[6]: Szedlmayer, M. and Kweon, C., "Effect of Altitude Conditions on Combustion and Performance of a Multi-Cylinder Turbocharged Direct-Injection Diesel Engine," SAE Technical Paper 2016-01-0742, 2016, doi:10.4271/2016-01-0742.

[7]: Wang, X., Ge, Y., Yu, L., Feng, X., “Comparison of combustion characteristics and brake thermal efficiency of a heavy-duty diesel engine fueled with diesel and biodiesel at high altitude”, Fuel, Volume 107, May 2013, Pages 852-858, https://doi.org/10.1016/j.fuel.2013.01.060

[8]: Zervas, E., „Impact of alititude on fuel consumption of a gasoline passenger car“, Fuel 2011

[9]: Shannak, B. A., Alhasan, M., „Effect of atmospheric altitude on engine performance“, Forschung im Ingenieurwesen 67 (2002)

[10]: Hashmi, K. and Radhakrishna, D., “Prediction of High Altitude Performance for UAV Engine”, SAE Technical Paper 2015-26-0207, 2015, doi:10.4271/2015-26-0207

[11]: Amiel, R. and Tartakovsky, L., “Effect of Flight Altitude on the Knock Tendency of SI Reciprocating Turbocharged Engines”, SAE Technical Paper 2016-32-0006, 2016, doi:10.4271/2016-32-0006.

[12]: Bell, A. „Modern SI Engine Control Parameter Responses and Altitude Effects with Fuels of Varying Octane Sensitivity“, SAE Technical Paper 2010-01-1454, 2010, doi:10.4271/2010-01-1454

[13]: Environmental Systems Research Institute, Inc., “hompage”, http://desktop.arcgis.com/de/arcmap/10.3/tools/spatial-analyst-toolbox/how-natural-neighbor-works.htm, accessed 13.08.2019

[14] Wolfram Research, Inc., „homepage“ http://mathworld.wolfram.com/VoronoiDiagram.html, accessed 13.08.2019

[15]: Pischinger, R., „Thermodynamik der Verbrennungskraftmaschine“, 3. Auflage, Wien [u.a.], Springer, 2009

[16] [ROTAX 912 UL]: Motorbeschreibung https://www.flyrotax.com/produkte/detail/rotax-912-ul-a-f.html; accessed 21.07.2019

[17]: Gamma Technologies LLC, „GT-Manual, Flow Theory Manual“ (Version 7.4, 2014)

[18]: Heywood, J. B., „Internal Combustion Engine Fundamentals“, New York, McGraw-Hill, 1988

[19]: Merker G. P., Schwarz, C., Teichmann, R., „Grundlagen Verbrennungsmotoren“, 5. Auflage, Vieweg+Teubner Verlag | Springer Fachmedien Wiesbaden GmbH 2011

[20]: Ward, D. T., Miley S, J,; Practical Flight Test Method for Determinign Reciprocating Engine Cooling Requirements, J Aircraft Vol. 21. N0 12, 1984

[21]: The MathWorks. Inc, “hompage”, https://de.mathworks.com/help/curvefit/interactive-curve-and-surface-fitting-.html, accessed 13.08.2019

[22]: Diamond Aircraft Industries, “Flughandbuch DA 20 KATANA”, Diamond Aircraft Industries, London, Ontario, Canada, 1996

5. DEFINITIONS

A	=	area
A(x,y)	=	surface area of Voronoi cell
c	=	coefficient
c_s	=	spring stiffness
d	=	distance / diameter
f(x,y)	=	data point
h	=	specific enthalpy / altitude
h_V	=	valve lift
I(x,y)	=	interpolation value
m	=	mass / Vibe exponent / exponent
$\dot{m}$	=	mass flow
M_{eff}	=	effective engine torque
n	=	engine speed
p	=	pressure / weighting factor
P	=	power
P_{eff}	=	effective Power
Q	=	heat
R_L	=	gas constant o fair
t	=	time
T	=	temperature
U	=	inner energy
V	=	volume
w(x,y)	=	weighting factor
W	=	work
x_{awb}	=	vibe factor
x,y	=	position of interpolation and grid points
y	=	lift
$\ddot{y}$	=	lift acceleration
α	=	heat transfer coefficient
η	=	efficiency
$\eta_{complete}$	=	fuel degree of conversion
κ	=	isentropic exponent
λ	=	air-fuel ratio
λ_a	=	volumetric efficiency
μ	=	flow coefficient
ρ	=	density
σ	=	density ratio
φ	=	throttle angle / crank angle
ψ	=	flow function
ω	=	angular speed

abbreviations:

a	=	outlet
B	=	burned fuel
BB	=	blow by
BMEP	=	break mean effective pressure
Br,ver	=	fuel evaporation
BSFC	=	break specific fuel consumption
CH	=	cylinder head
CW	=	cooling water
D	=	cross section carburetor
e	=	inlet
eff	=	effective
ex	=	exhaust gas
F	=	fuel
Gas	=	in cylinder gas
geo	=	geometrical
ICE	=	internal combustion engine
In	=	inlet side
MTOM	=	maximum take-off mass
MTOP	=	maximum take-off power
ref	=	reference
SL	=	sea level
sys	=	system
TDC	=	top dead center
theo	=	theoretical
TP	=	throttle angle
u	=	environment
ver	=	evaporation
Wa	=	outside wall
Wi	=	inside wall
Wo	=	Woschni
WP	=	work package